Role of kinase-independent and -dependent functions of FAK in endothelial cell survival and barrier function during embryonic development

Xiaofeng Zhao,[1,3] Xu Peng,[1] Shaogang Sun,[1] Ann Y.J. Park,[1] and Jun-Lin Guan[1,2]

[1]Division of Molecular Medicine and Genetics, Department of Internal Medicine and [2]Department of Cell and Developmental Biology, University of Michigan, Ann Arbor, MI 48109
[3]Graduate Field of Biochemistry, Molecular, and Cell Biology, Cornell University, Ithaca, NY 14853

Focal adhesion kinase (FAK) is essential for vascular development as endothelial cell (EC)–specific knockout of FAK (conditional FAK knockout [CFKO] mice) leads to embryonic lethality. In this study, we report the differential kinase-independent and -dependent functions of FAK in vascular development by creating and analyzing an EC-specific FAK kinase-defective (KD) mutant knockin (conditional FAK knockin [CFKI]) mouse model. CFKI embryos showed apparently normal development through embryonic day (E) 13.5, whereas the majority of CFKO embryos died at the same stage. Expression of KD FAK reversed increased EC apoptosis observed with FAK deletion in embryos and in vitro through suppression of up-regulated p21. However, vessel dilation and defective angiogenesis of CFKO embryos were not rescued in CFKI embryos. ECs without FAK or expressing KD FAK showed increased permeability, abnormal distribution of vascular endothelial cadherin (VE-cadherin), and reduced VE-cadherin Y658 phosphorylation. Together, our data suggest that kinase-independent functions of FAK can support EC survival in vascular development through E13.5 but are insufficient for maintaining EC function to allow for completion of embryogenesis.

Introduction

Endothelial cells (ECs) play central roles in the development of vasculature essential for embryogenesis (Folkman, 1995; Dvorak, 2003). The survival and function of ECs are regulated by complex interactions among growth factor receptors, integrin receptors, and their extracellular ligands, which can trigger multiple intracellular signaling pathways through cytoplasmic kinases, small GTPases, and other adaptor molecules. FAK is a major mediator of signal transduction by integrins and also participates in signal transduction by growth factor receptors such as VEGF receptors in ECs (Schaller, 2001; Parsons, 2003; Schlaepfer and Mitra, 2004; Cohen and Guan, 2005; Siesser and Hanks, 2006). A role of FAK in vascular development has been established by recent findings that EC-specific deletion of FAK results in embryonic lethality caused by decreased survival and other defects of ECs (Shen et al., 2005; Braren et al., 2006). However, little is known about the mechanisms by which FAK exerts its regulatory functions through multiple target molecules and signaling pathways in embryonic development.

Recent studies suggest that FAK functions not only as a kinase but also through its kinase-independent activities in different cellular processes (Shen et al., 2005; Lim et al., 2008). Nevertheless, whether kinase activity of FAK is required for survival and/or function of ECs in vascular development and embryogenesis is not clear. In this study, we address this issue directly by creating a FAK knockin mouse model with kinase-defective (KD) mutant allele in endogenous FAK gene in ECs. Analysis of the EC-specific FAK mutant knockin embryos and isolated ECs revealed both kinase-independent and -dependent functions of FAK in EC survival and their barrier function, respectively, which are required for vascular development and embryogenesis at different stages.

Correspondence to Jun-Lin Guan: jlguan@umich.edu

Abbreviations used in this paper: CFKI, conditional FAK knockin; CFKO, conditional FAK knockout; EC, endothelial cell; FRNK, FAK-related nonkinase; KD, kinase defective; VE-cadherin, vascular endothelial cadherin.

The Rockefeller University Press $30.00
J. Cell Biol. Vol. 189 No. 6 955–965
www.jcb.org/cgi/doi/10.1083/jcb.200912094

Table I. **Genotypes of progeny from crosses to generate CFKI and CFKO mice**

Genotypes	E12.5	E13.5	E14.5	E15.5	E16.5	Born
Progeny from crosses between *FAK*$^{+/KD}$;Tie2-Cre and *FAK*$^{flox/flox}$ mice						
flox/KD	7	36	25	24	10	79
flox/KD;Tie2-Cre (CFKI)	9	40	9	4	1	0
flox/+	8	35	27	19	12	92
flox/+;Tie2-Cre	6	37	30	19	10	85
Progeny from crosses between *FAK*$^{+/flox}$;Tie2-Cre and *FAK*$^{flox/flox}$ mice						
flox/flox	12	33	13	ND	ND	72
flox/flox;Tie2-Cre (CFKO)	12	15	0	ND	ND	0
flox/+	12	37	14	ND	ND	71
flox/+;Tie2-Cre	16	40	16	ND	ND	68

Results and discussion

Generation of KD FAK mutant knockin mice

To study the potential role of kinase-independent functions of FAK in vivo, we generated a KD mutant FAK allele in the endogenous FAK gene using a gene knockin approach via homologous recombination. The K454 to R mutation abolishing FAK kinase activity was created in exon 16 of FAK genomic DNA, and a targeting vector containing the mutated exon 16 and a neomycin cassette (KD[neo] allele) was used to generate mutant mice containing the knockin mutant allele (Fig. S1), as described in Materials and methods. All *FAK*$^{+/KD}$ mice were viable, fertile, and indistinguishable from wild-type mice, confirming that one functional FAK allele is sufficient for normal mouse development and that the KD mutant allele (in the endogenous gene and not overexpressed) did not exhibit any dominant-negative effect severe enough to result in embryonic lethality and/or sterility for the mice. Mating between heterozygous *FAK*$^{+/KD}$ mice yielded wild-type (i.e., *FAK*$^{+/+}$) and *FAK*$^{+/KD}$ mice at the expected 1:2 Mendelian ratio, but no homozygous FAK knockin (i.e., *FAK*$^{KD/KD}$) mice were detected after >400 pups were screened (unpublished data). Analysis of embryos from intercrosses of *FAK*$^{+/KD}$ mice did not detect any live *FAK*$^{KD/KD}$ embryos beyond embryonic day (E) 10.5 (unpublished data). These results suggested that the kinase activity of FAK is required for embryogenesis and that the kinase-independent functions of FAK are not sufficient to rescue the early embryonic lethality of FAK KO mice.

KD FAK is sufficient to rescue vascular developmental defects in conditional FAK knockout (CFKO) mice through E13.5

To investigate the potential role of kinase-independent functions of FAK in vascular development in vivo, we crossed *FAK*$^{+/KD}$ mice to Tie2-Cre mice expressing Cre recombinase in ECs (Koni et al., 2001) to generate *FAK*$^{+/KD}$;Tie2-Cre mice, which were then crossed with *FAK*$^{flox/flox}$ (Shen et al., 2005) mice to produce *FAK*$^{flox/KD}$;Tie2-Cre mice (Table I). The *FAK*$^{flox/KD}$;Tie2-Cre mice expressed only KD FAK protein in ECs from the knockin KD mutant allele (flox allele was converted to the deleted allele by Tie2-Cre) but contained functional FAK (i.e., the flox allele) in other cells, and therefore were designated as conditional FAK knockin (CFKI) mice. Parallel crosses between *FAK*$^{flox/+}$;Tie2-Cre and *FAK*$^{flox/flox}$ were also performed to generate *FAK*$^{flox/flox}$;Tie2-Cre mice (i.e., CFKO mice in which both FAK alleles were converted to the deleted allele, thus inactivating FAK completely in ECs; Shen et al., 2005) for comparison with CFKI mice. As shown in Table I, both CFKI and CFKO embryos were recovered at Mendelian ratios at E12.5. At E13.5, CFKI embryos were still at Mendelian ratio, and the majority of the embryos appeared normal in gross appearance (Fig. 1 A). In contrast, much fewer CFKO embryos than Mendelian ratio were recovered, and most showed various vascular defects, including multifocal superficial hemorrhages and edema, as described previously (Shen et al., 2005). At E14.5 and later, reduced CFKI embryos were found, and surviving embryos exhibited various vascular defects too, whereas no live CFKO embryos were present at these stages. Lastly, we did not detect any live pups for either CFKI or CFKO mice out of >200 examined.

Consistent with observation of gross morphology, histological examination also showed rescue of various vascular defects in CFKI embryos. As shown in Fig. 1 B, perivascular hemorrhages were found in the CFKO embryos (b), whereas all red blood cells were restricted inside the intact vessels in the control embryos (a), as shown previously (Shen et al., 2005). Interestingly, this phenotype was not found in CFKI embryos (Fig. 1 B, c), suggesting that these vascular defects were rescued by the kinase-independent functions of FAK. The fetal placental tissues increase noticeably with significant vascularization of the vital organ in midgestation (Watson and Cross, 2005). As shown previously (Shen et al., 2005), defective vascularization caused significant decrease in the thickness of the labyrinth layer of CFKO placenta compared with control placenta (Fig. 1 C). Analysis of CFKI placenta showed restored thickness of their labyrinth layer, suggesting that the kinase-independent functions of FAK were able to support placenta vascularization through E13.5. Consistent with this, the lack of vessels containing nucleated red blood cells (i.e., fetal vessels; Fig. 1 B, d–f, arrows) in CFKO placenta was also rescued in CFKI placenta.

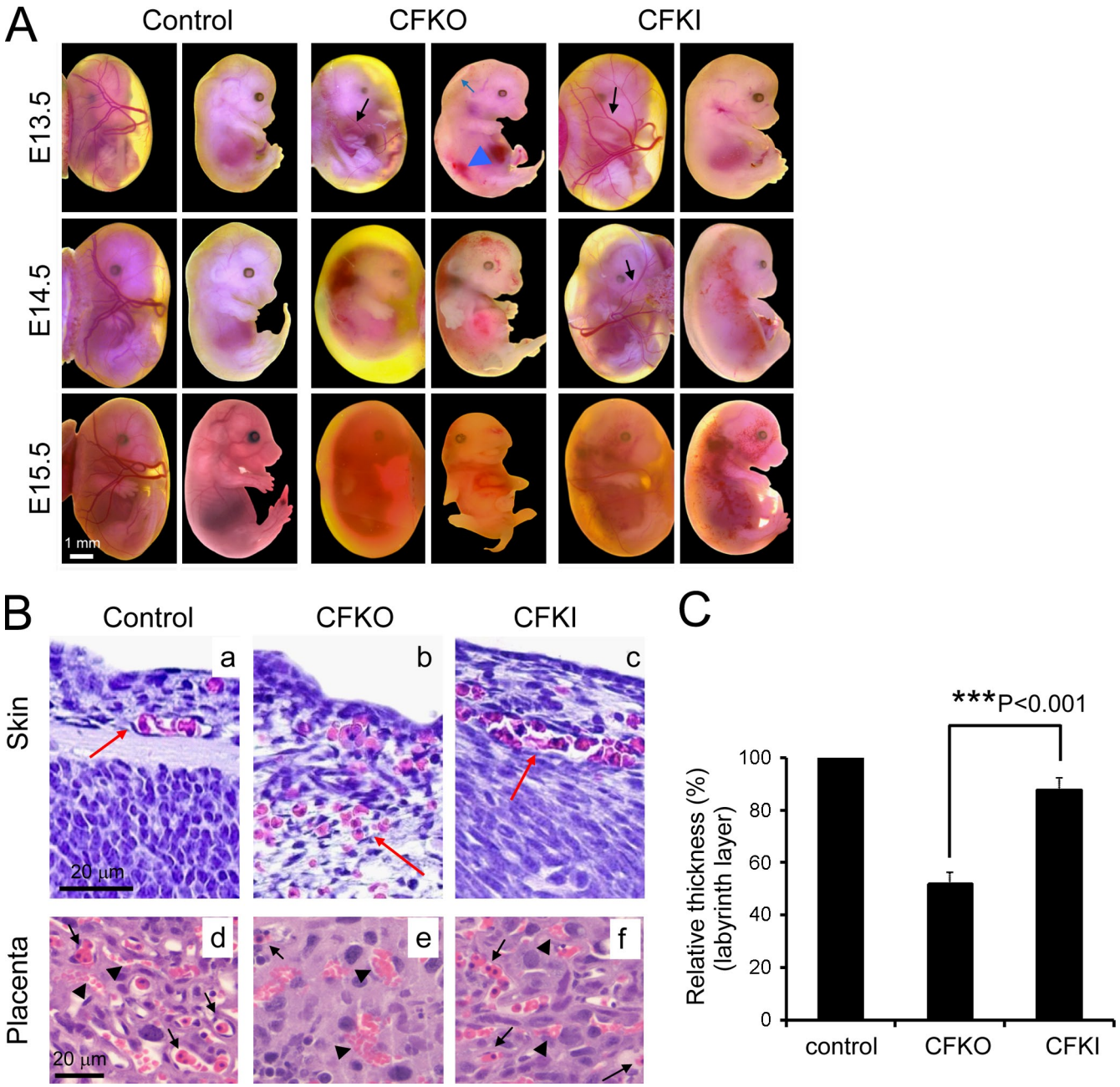

Figure 1. **Kinase-independent functions of FAK are sufficient to support normal embryonic development through E13.5.** (A) Gross examination of whole embryos at various stages with or without intact yolk sac. Note the significantly reduced vascular network in CFKO embryos at E13.5, which was restored in CFKI embryos (arrows). The edema (blue arrow) and hemorrhages (blue arrowhead) observed in CFKO at E13.5 are also absent in CFKI embryos. The CFKO embryos found at E14.5 and E15.5 were smaller and with marked abnormalities caused by embryonic death, whereas a significant fraction of CFKI embryos were alive with more limited defects. (B) H&E staining of skin and labyrinth layer of placenta sections of control, CFKO, and CFKI embryos at E13.5. In a–c, arrows mark red blood cells within vessels for control and CFKI embryos (a and c) and outside of vessels because of a hemorrhage in CFKO embryos (b). In d–f, note the reduced number of vessels that contain the nucleated red blood cells from fetal embryos (arrows) in CFKO mice (e) compared with control and CFKI mice (d and f). Arrowheads mark maternal vessels containing enucleated red blood cells that are present in all three samples. (C) Placenta sections from control, CFKO, and CFKI embryos at E13.5 were stained with H&E. Mean ± SEM of calculated thickness of labyrinth layer from three independent experiments in multiple fields is shown as a percentage of the value in control embryos.

Together, these results suggest that kinase-independent functions of FAK are able to support vascular development through E13.5 by rescuing the deficiency caused by deletion of FAK in ECs. They also indicate that the kinase activity of FAK is required for late stages of vascular development to support the completion of embryogenesis.

KD FAK promotes EC survival through regulation of p21

Because the reduced EC survival has been suggested as a major cause of vascular defects in CFKO mice (Shen et al., 2005; Braren et al., 2006), we examined whether KD FAK can rescue the increased EC apoptosis in CFKI embryos. As shown in

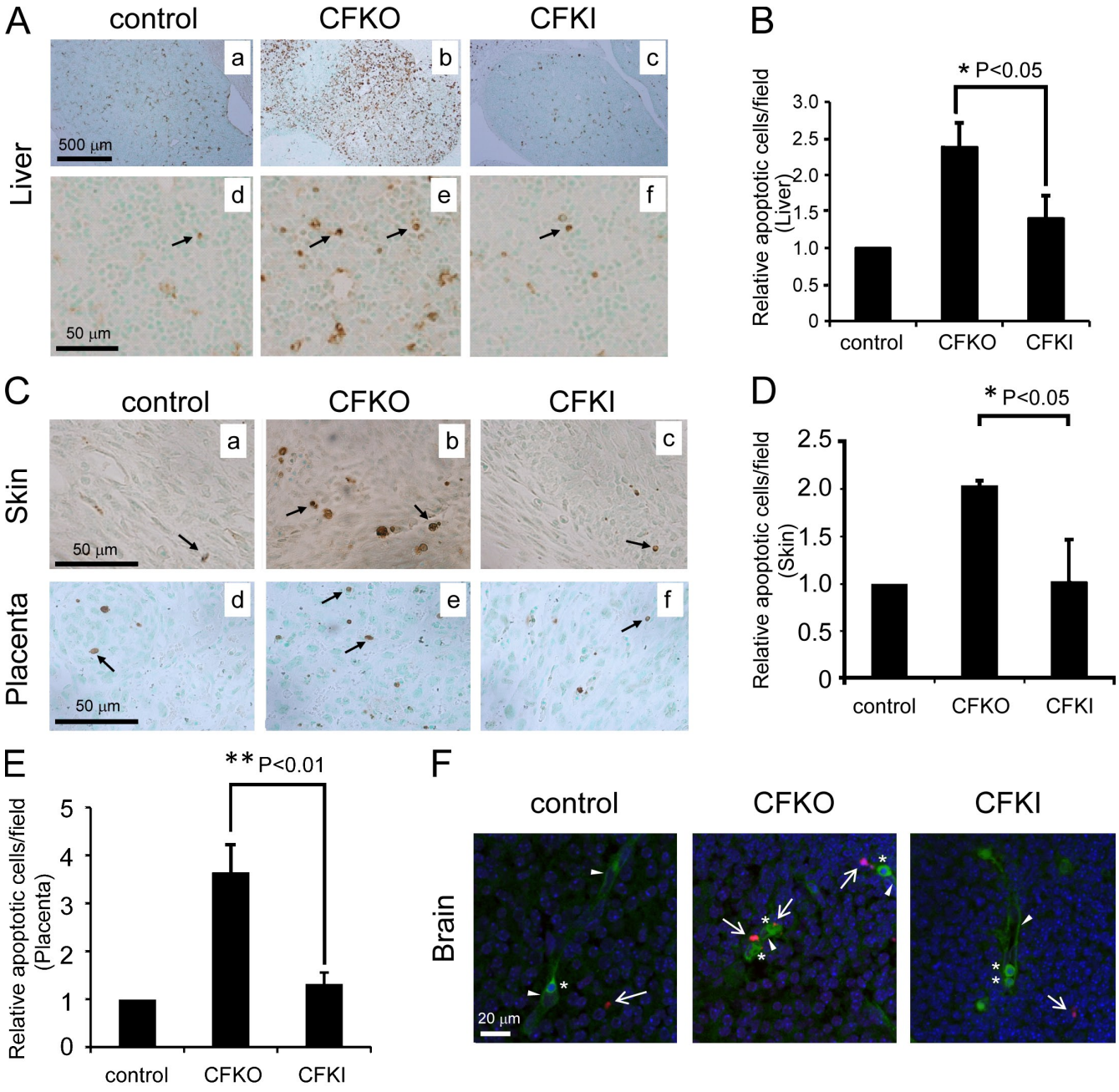

Figure 2. **Kinase-independent functions of FAK rescue the increased apoptosis induced by FAK deletion.** (A–E) Sections from livers, skins, or placenta of control, CFKO, or CFKI embryos at E13.5 were analyzed by TUNEL assays. (A and C) Representative fields with arrows marking apoptotic cells. (B, D, and E) Mean ± SEM of relative number of apoptotic cells per field from three experiments. (F) Brain sections from control, CFKO, or CFKI embryos at E13.5 were analyzed by TUNEL assays followed by staining using PECAM-1 and Hoechst. ECs and blood cells (both green) are marked by arrowheads and asterisks, respectively. Apoptotic cells are marked by arrows (red). Note the presence of apoptotic ECs in the vessel of CFKO embryos but not control or CFKI embryos.

Fig. 2 (A and B), increased apoptosis was found in the liver of CFKO embryos (b and e) compared with control embryos (a and d). Interestingly, the liver of CFKI embryos showed only a slight increase in apoptosis (c and f). The increased apoptosis in the placenta and skin of CFKO embryos was also rescued in CFKI embryos (Fig. 2, C–E). Double staining of brain sections revealed the presence of apoptotic ECs in the blood vessel of CFKO embryos but not CFKI or control embryos (Fig. 2 F). Similar results were found in skin sections (Fig. S2 A and not depicted). These results suggest that KD FAK was able to rescue the defective survival of ECs caused by deletion of FAK in embryos.

To further define the role of kinase-independent functions of FAK in EC-autonomous survival, ECs were isolated from $FAK^{flox/flox}$, $FAK^{flox/KD}$, and $FAK^{+/flox}$ mice (Fig. S2, B and C) and infected by recombinant adenoviruses encoding Cre (Ad-Cre) to delete floxed FAK allele (Fig. S2 D), as described previously (Shen et al., 2005). As expected, Ad-Cre infection of $FAK^{flox/flox}$ ECs but not ECs from $FAK^{+/flox}$ mice led to their increased apoptosis (Fig. 3, A and B). Interestingly, the presence

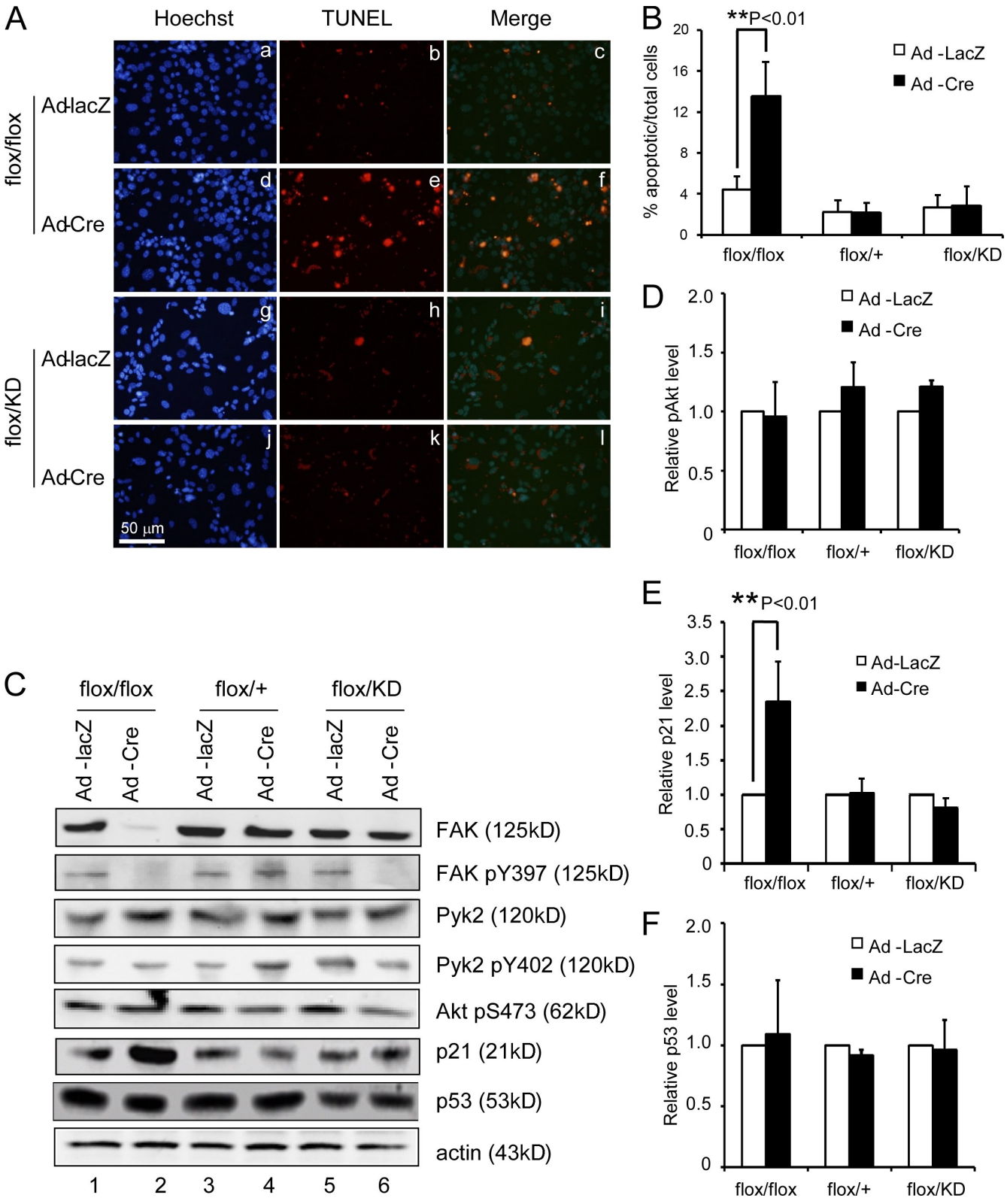

Figure 3. **Kinase-independent functions of FAK suppress the increased apoptosis induced by FAK deletion in vitro.** ECs from $FAK^{flox/flox}$, $FAK^{+/flox}$, and $FAK^{flox/KD}$ mice were infected with Ad-Cre to delete the floxed FAK allele or Ad-lacZ as a control, as indicated. (A and B) The infected cells were then stained by Hoechst and analyzed for apoptosis using TUNEL assay. (A) Representative fields for ECs from $FAK^{flox/flox}$ and $FAK^{flox/KD}$ mice stained by Hoechst (a, d, g, and j) or TUNEL (b, e, h, and k) or merged images (c, f, i, and l). (B) Mean ± SEM from three experiments. (C) Aliquots of lysates from the infected cells were analyzed by Western blotting using various antibodies, as indicated. (D–F) The intensity of the pAkt (D), p21 (E), and p53 (F) bands was quantified from three independent experiments by densitometry. The mean ± SEM of relative intensity (normalized to lacZ-infected cells) is shown.

of KD FAK in Ad-Cre–infected ECs from $FAK^{flox/KD}$ mice reversed the increased apoptosis, suggesting that kinase-independent functions of FAK are sufficient for EC survival, which may account for the rescued vascular development in CFKI embryos through E13.5.

To study possible mechanisms by which KD FAK rescued the increase of EC apoptosis in FAK-null ECs, lysates were prepared and analyzed for FAK downstream targets. As shown in Fig. 3 C, deletion of flox FAK by Ad-Cre abolished FAK expression in ECs from $FAK^{flox/flox}$ mice (lanes 1 and 2) but did not affect FAK expression in ECs from $FAK^{+/flox}$ and $FAK^{flox/KD}$ mice because of the remaining wild-type or KD allele (lanes 3–6). Similar FAK autophosphorylation at Y397 was detected in ECs infected by Ad-lacZ and $FAK^{+/flox}$ ECs infected by Ad-Cre (Fig. 3 C, lanes 1 and 3–5). As expected, KD FAK in $FAK^{flox/KD}$ ECs infected by Ad-Cre was not autophosphorylated at Y397 (Fig. 3 C, lane 6). No significant difference in the expression or activation of FAK-related kinase Pyk2 was observed in ECs with FAK deletion or expression of KD FAK. Akt has been implicated in mediating FAK regulation of cell survival in previous studies (Frisch et al., 1996; Chan et al., 1999; Sonoda et al., 2000). However, activation of Akt was not changed in ECs with FAK deletion or with only KD FAK compared with controls (Fig. 3, C and D). In contrast, we found that p21 was increased upon deletion of FAK, but infection of ECs from $FAK^{flox/KD}$ or $FAK^{+/flox}$ mice by Ad-Cre did not lead to an increase of p21 (Fig. 3, C and E). Analysis of the mRNAs from these ECs by quantitative RT-PCR showed an ∼2.5-fold up-regulation of p21 mRNA upon deletion of FAK, whereas no differences were found in ECs from $FAK^{+/flox}$ or $FAK^{flox/KD}$ mice infected by Ad-Cre (Fig. S2 E). Moreover, inhibition of FAK by FAK-related nonkinase (FRNK) also increased p21 expression in ECs (Fig. S2 F), suggesting that this is not a secondary consequence of FAK deletion. Given the role of increased p21 in apoptosis (Sekiguchi and Hunter, 1998; Fotedar et al., 1999), these results suggest that the up-regulation of p21 may contribute to increased EC apoptosis upon FAK deletion and that the kinase-independent functions of FAK could rescue EC apoptosis and defective vascular development through controlling p21 expression.

Lim et al. (2008) recently showed that FAK could facilitate p53 turnover in the nucleus through its FERM domain in a kinase-independent manner. However, no difference in the expression of p53 was observed in ECs upon FAK deletion or expression of KD FAK (Fig. 3, C and F). Although we cannot exclude the possibility that the activity of p53 (rather than its expression level) could be altered to regulate p21 in ECs, our current data suggest potentially p53-independent mechanisms of p21 regulation by FAK in a kinase-independent manner.

Defective angiogenesis and dilated vessels in CFKI embryos

We next examined the vascular defects besides EC apoptosis, which are not rescued by KD FAK and thus could be responsible for the later lethality of CFKI embryos (although not crucial for embryogenesis through E13.5). Consistent with previous findings (Shen et al., 2005; Braren et al., 2006), fewer blood vessels were found in the brain from CFKO embryos compared with control embryos (Fig. 4, A and B). CFKI embryos also showed a decreased number of vessels, suggesting that kinase-independent functions of FAK were not sufficient to rescue the angiogenesis defects upon FAK deletion. In addition to the reduced vessel numbers, we observed evident dilation of vessels in both CFKO and CFKI embryos compared with control embryos (Fig. 4, A and C). The defective vessel dilations were also found in other organs such as the spinal cord and skins of CFKO and CFKI embryos (Fig. 4, D–F). Examination of the embryos by whole-mount staining of PECAM-1 showed the enlarged vessels in CFKO embryos as well as CFKI embryos, although to a lesser extent, compared with control embryos at E12.5 (Fig. S3 A). Together, these results suggest that the deficiency in the blood vessels, as exhibited by their dilation and reduced angiogenesis, was not rescued by KD FAK and could be responsible for the embryonic lethality of the CFKI embryos, which were associated with signs of leaky vasculature such as multifocal hemorrhages and edema at later developmental stages.

FAK kinase activity is required for maintaining EC integrity and vascular endothelial cadherin (VE-cadherin) phosphorylation

To explore the potential mechanisms of the abnormal vascular integrity in CFKO and CFKI embryos, we examined the possible regulation of EC permeability by FAK by measuring transport of FITC-dextran through a confluent monolayer of isolated ECs grown on Transwell plates, as described previously (Moldobaeva and Wagner, 2002). As shown in Fig. 5 A, deletion of FAK in $FAK^{flox/flox}$ ECs by Ad-Cre increased their permeability, whereas infection of $FAK^{+/flox}$ ECs by Ad-Cre had no effect. ECs with KD FAK (Ad-Cre infection of $FAK^{flox/KD}$ ECs) also showed increased permeability, indicating that kinase activity of FAK was required to maintain the integrity of ECs. These results suggest that FAK regulates EC permeability and that the abnormalities in EC barrier function may contribute to the compromised integrity of the blood vessels, which, although they did not affect embryonic development through E13.5, manifested in the severe hemorrhages and edema in the later stage of embryogenesis, leading to the lethality of CFKI embryos.

VE-cadherin is a major mediator of cell–cell adhesion of ECs and is responsible for regulation of their permeability under a variety of conditions (Gavard and Gutkind, 2006; Dejana et al., 2008). To understand regulation of EC permeability by FAK, the expression and distribution of VE-cadherin was examined in $FAK^{flox/flox}$ and $FAK^{flox/KD}$ ECs infected by Ad-lacZ or Ad-Cre (Fig. 3 C and Fig. S2 D). As shown in Fig. 5 B, ECs infected by Ad-lacZ showed smooth and continuous staining of VE-cadherin on the membrane (a and c). In contrast, upon deletion of FAK in $FAK^{flox/flox}$ ECs by Ad-Cre infection, the VE-cadherin exhibited a considerably different pattern with discontinuous staining and a more zigzag pattern (Fig. 5 B, b). Similarly, a disrupted pattern of VE-cadherin on the plasma membrane was observed in $FAK^{flox/KD}$ ECs after Ad-Cre infection (Fig. 5 B, d). In contrast, no apparent differences in distribution of either β-catenin or p120-catenin were observed in

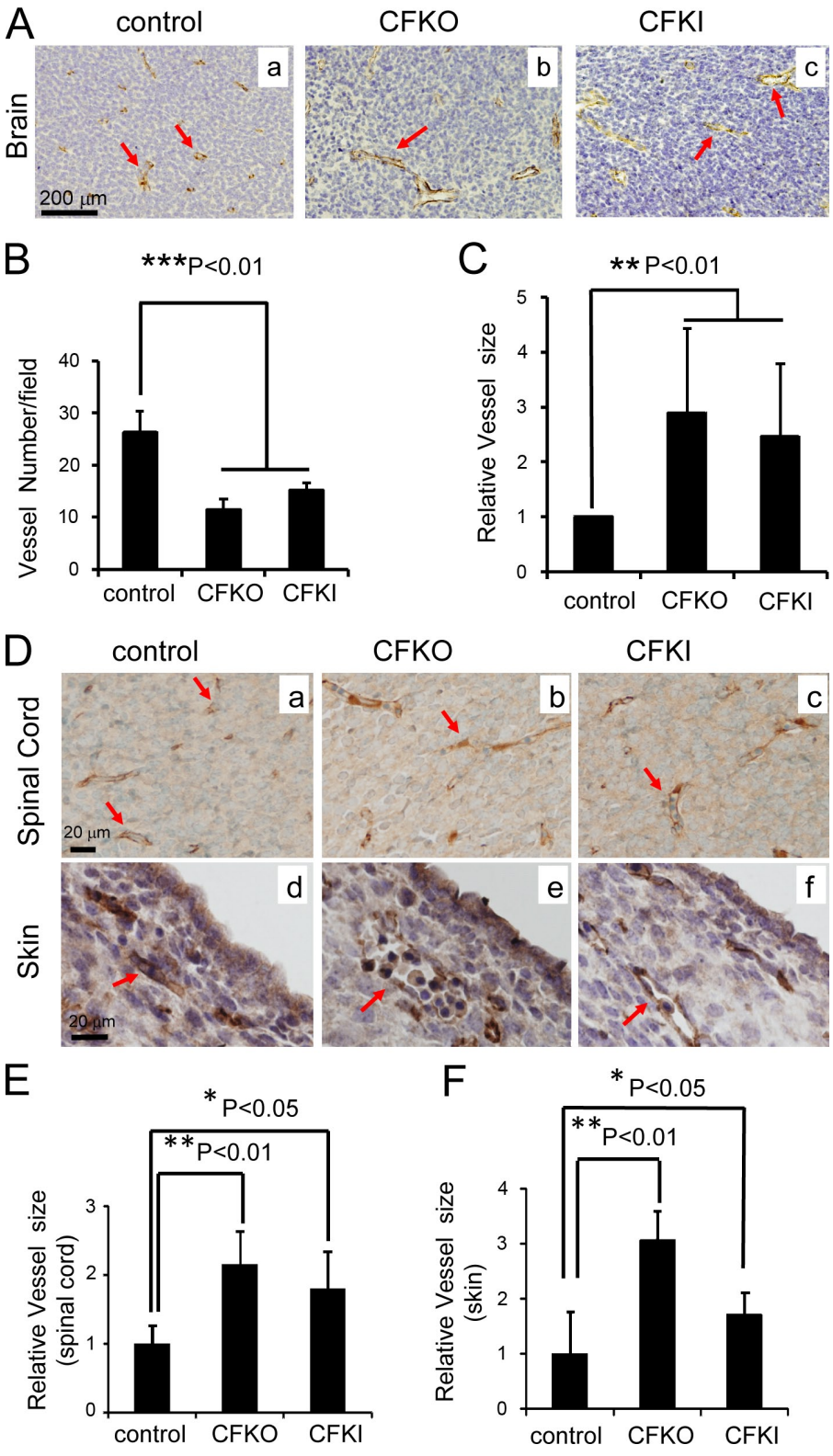

Figure 4. **KD FAK is unable to rescue the reduced angiogenesis and vessel dilation caused by FAK deletion.** (A) Brain sections from control, CFKO, and CFKI embryos at E13.5 were stained with anti–PECAM-1. Note the reduced density and dilated vessels (arrows) in CFKO and CFKI embryos (b and c) compared with control embryos (a). (B) Mean ± SEM of vessel numbers per field from three independent experiments. (C) Mean ± SEM of relative vessel size normalized to the value in control embryos from three independent experiments. (D) Sections from spinal cords (a–c) or skin (d–f) of control, CFKO, and CFKI embryos at E13.5 were stained with anti–PECAM-1. Vessels are marked by arrows. (E and F) Mean ± SEM of relative vessel size normalized to the value in control embryos from three independent experiments.

these cells (Fig. S3 B). As the zigzag pattern of VE-cadherin distribution at cell–cell junctions has been correlated with increased permeability of ECs (Lampugnani et al., 1995; Esser et al., 1998; Lampugnani et al., 2002), these results suggest that FAK may affect EC integrity through its regulation of VE-cadherin in a kinase-dependent manner.

Tyrosine phosphorylation of VE-cadherin has been shown to regulate its functions in cell–cell adhesion and vascular permeability previously (Esser et al., 1998; Allingham et al., 2007; Turowski et al., 2008). Therefore, we examined phosphorylation of Y658 of VE-cadherin, which could increase EC permeability by decreasing VE-cadherin association with p120-catenin

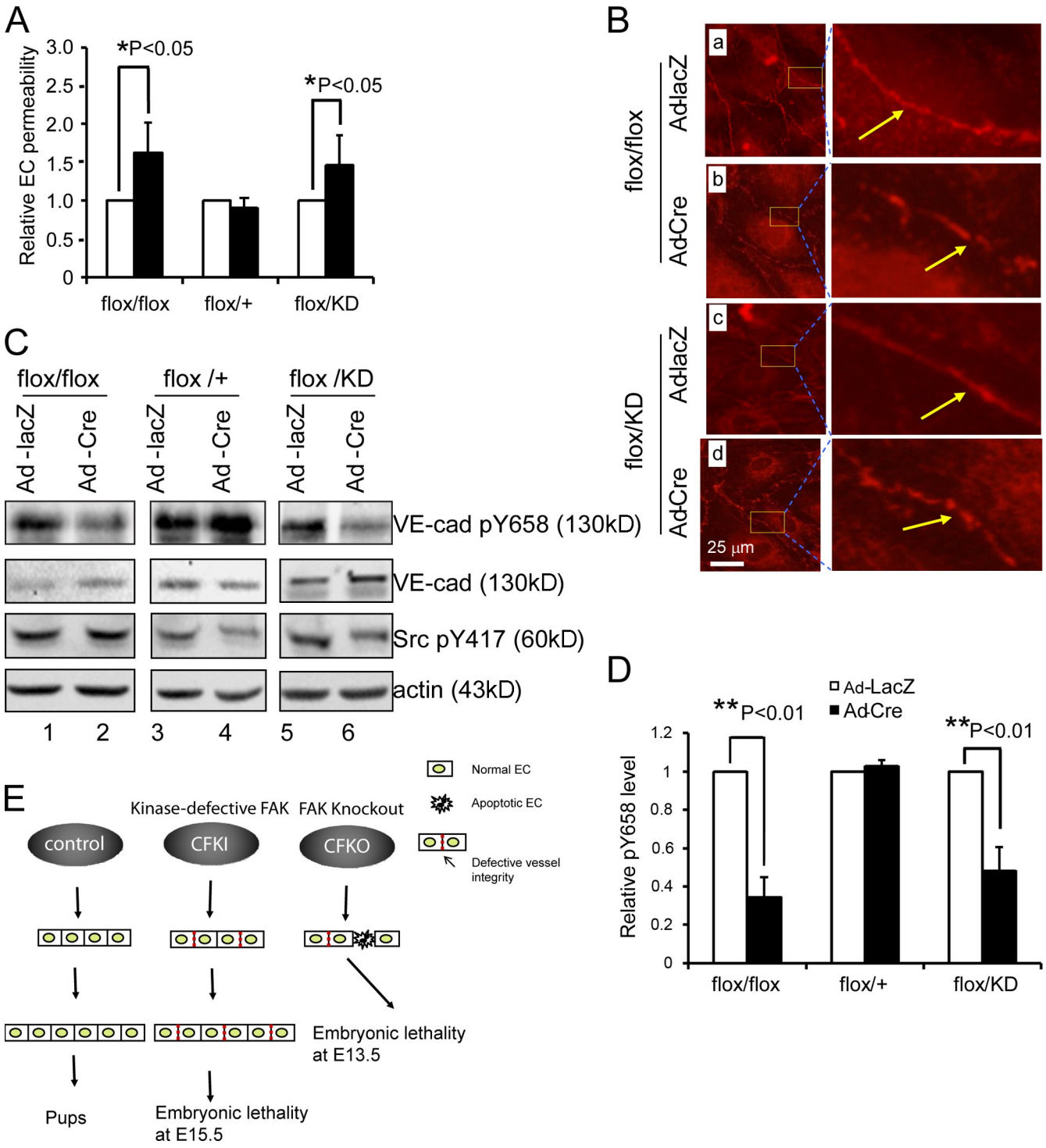

Figure 5. **Normal EC barrier function and distribution and Y658 phosphorylation of VE-cadherin requires FAK kinase activity.** ECs from *FAK*$^{flox/flox}$, *FAK*$^{+/flox}$, and *FAK*$^{flox/KD}$ mice were infected with Ad-Cre (closed bars) to delete the floxed FAK allele or Ad-lacZ (open bars) as a control, as indicated. (A) The infected cells were analyzed for their barrier function using Transwell assay as described in Materials and methods. The mean ± SEM of relative EC permeability (normalized to lacZ-infected cells) is shown. (B) Representative images of immunofluorescent staining by anti–VE-cadherin for infected cells from *FAK*$^{flox/flox}$ and *FAK*$^{flox/KD}$ mice. Arrows mark the discontinuous pattern of VE-cadherin distribution in cells infected with Ad-Cre. (C) Aliquots of lysates from the infected cells were analyzed by Western blotting using various antibodies, as indicated. (D) The intensity of the VE-cadherin pY658 bands was quantified from three independent experiments by densitometry. The mean ± SEM of relative intensity (normalized to lacZ-infected cells) is shown. (E) A working model of kinase-dependent (absent in both CFKI and CFKO embryos) and -independent (present in CFKI embryos) functions of FAK in vascular development.

(Potter et al., 2005). To our surprise, infection of $FAK^{flox/flox}$ or $FAK^{flox/KD}$ ECs but not $FAK^{+/flox}$ ECs by Ad-Cre reduced Y658 phosphorylation rather than increased it (Fig. 5, C and D). Y658 is a site of phosphorylation by Src upon VEGF stimulation (Potter et al., 2005), which is also dependent on Pyk2 in the phosphorylation induced by leukocyte binding through ICAM1 (Allingham et al., 2007). Our results suggest that the basal phosphorylation of this residue also requires FAK kinase activity. Interestingly, similar activation levels of Src were found in ECs without FAK or KD FAK only, compared with control cells (Fig. 5 C), suggesting that FAK may promote Src phosphorylation of Y658 through a scaffolding function, which requires autophosphorylation of Y397 (Fig. 3 C), rather than by increasing Src activity by itself. Interestingly, a recent study showed that deletion of exon 15 (containing Y397) of FAK also caused late embryonic lethality with multiple vascular defects similar to those in CFKI embryos (Corsi et al., 2009), suggesting that defective basal Y658 phosphorylation in VE-cadherin mediated by FAK could also be responsible in these embryos.

Conclusions

By creating a KD FAK knockin allele in mice, we identified both kinase-independent and -dependent functions of FAK important in vascular development, as shown in a working model (Fig. 5 E). Deletion of FAK in ECs results in their increased apoptosis and more subtle defects like increased permeability, leading to embryonic lethality around E13.5. The expression of KD FAK was able to rescue the increased EC apoptosis through regulation of p21 by kinase-independent functions of FAK to allow further development of the embryos beyond this stage. However, FAK kinase activity is required for maintaining normal barrier function of ECs through proper phosphorylation of Y658 of VE-cadherin. As CFKI embryos progressed in development, these subtle vascular defects led to lethality around E15.5, possibly as a result of the increased reliance of embryos on vessel integrity as they got bigger, the increased severity of defects in vessel integrity, or both.

Tyrosine kinases play essential roles in many biological processes, including vascular development, and identification of their targets has been the focus of studies over the years (for reviews see Hunter, 2009; Pawson and Kofler, 2009). Our results demonstrating a kinase-independent function of FAK in vascular development raise the possibility of such mode of actions by other tyrosine kinases in development and diseases. Therefore, future investigation on such possibilities (especially in the context of in vivo developmental or disease models) will complement the efforts in identifying key substrates of tyrosine kinases to provide a better understanding of tyrosine kinase signaling mechanisms. Future studies will also be necessary to clarify the specific FAK kinase–independent and –dependent downstream pathways in the regulation of crucial targets involved in ECs and perhaps other cell types in embryogenesis and other biological processes. The direct demonstration of both kinase-independent and -dependent functions of FAK in vivo highlights the necessity to develop drugs that can inhibit all of FAK functions beyond the currently available kinase inhibitors for FAK (Halder et al., 2007; Slack-Davis et al., 2007; Roberts et al., 2008) in the treatment of cancer and possibly other diseases.

Materials and methods

Construction of the targeting vector and generation of CFKI mice

Based on available mouse genome sequences in the Ensembl database, an isogenic 129SvJ mouse BAC genomic clone containing FAK exon 16 (where the key K454 residue is encoded) and flanking sequences were obtained from BACPAC Resources Center. The presence of exon 16 in the BAC clone was verified by PCR using two pairs of primers surrounding exon 16 as well as Southern blotting. A targeting vector containing a mutated exon 16 (K454 to R) and a neomycin cassette was then constructed for homologous recombination (Fig. S1 A).

Gene targeting in 129P2/OlaHsd-derived E14Tg2a mouse embryonic stem cells (Skarnes, 2000) was performed as described previously (Kendall et al., 1995) with the use of ESGRO (Millipore). Chimeric mice were identified by coat color and then bred to C57BL/6J mice. Transmission of the germ line was identified by PCR (see next section) and confirmed by Southern blotting. Heterozygous targeted mice bearing the KD[neo] allele ($FAK^{+/KD[neo]}$ mice) were obtained and then crossed with EIIa-Cre mice (The Jackson Laboratory), which express Cre in the very early stage of embryogenesis (Lakso et al., 1996), to delete the neomycin cassette to avoid its possible interference with FAK gene expression. The progenies with neomycin cassette removed ($FAK^{+/KD}$;EIIa-Cre mice) were crossed with C57BL/6J mice to segregate the FAK KD allele from the heterozygote EIIa-Cre transgene. The resulting heterozygous FAK knockin mice ($FAK^{+/KD}$ mice) were identified by PCR analysis and confirmed by sequencing of tail DNA.

Tie2-Cre transgenic mice and CFKO mice have been described previously (Koni et al., 2001; Shen et al., 2005). All mice used in this study were bred and maintained at the University of Michigan under specific pathogen-free conditions in accordance with institutional guidelines.

Genotyping by PCR

Mice and embryos were genotyped by PCR analysis of genomic DNA. Isolation of genomic DNA was described previously (Chiang et al., 2000). Primers used to genotype flox and Δ FAK alleles were 5′-GCTGATGTCCCAAGCTATTCC-3′ and 5′-AGGGCTGGTCTGCGCTGACAGG-3′, as described previously (Shen et al., 2005). Primers used to genotype the FAK KD knockin allele were P1 5′-TCAACAGCATGTAACTTCCC-3′ and P2 5′-GGCATTCCAGTGCAAAACAC-3′ shown in Fig. S1 A. PCR was performed for 30 cycles of 94°C for 3 min, 67°C (for flox allele) or 60°C (for KD allele) for 2 min, and 72°C for 4 min. CreF (5′-GCAGAACCTGAAGATGTTCGCGATTA-3′) and CreR (5′-TCTCCCACCGTCAGTACGTGAGATATC-3′) primers were used to detect the Cre transgene, which was performed for 35 cycles of 95°C for 30 s, 60°C for 30 s, and 72°C for 30 s.

Morphological, histological, and immunohistochemical analysis

Timed matings were set up between male $FAK^{+/KD}$;Tie2-Cre and female $FAK^{flox/flox}$ mice to generate CKFI and control mice or male $FAK^{+/flox}$;Tie2-Cre and female $FAK^{flox/flox}$ mice to generate CFKO and control mice, respectively. Embryos, yolk sacs, and placenta were harvested between E12.5 and E15.5, fixed in 4% PFA in PBS at 4°C for 4–16 h, and transferred to 70% ethanol. They were examined for gross morphology and photographed on a dissecting microscope (model S6D; Leica) with a progressive 3CCD camera (Sony) and Image-Pro Plus version 3.0.00.00 (Media Cybernetics) at RT. The embryos and placenta were embedded in paraffin, sectioned (5 µm), and stained with hematoxylin and eosin (H&E) or nuclear dye Hoechst 33258 (Sigma-Aldrich) or used for immunohistochemistry. The slides were examined under a microscope (model BX41; Olympus) with UplanF1 10× NA 0.3 or UplanF1 20× NA 0.5 objective lenses at RT, and the images were captured using a camera (model DP70; Olympus) with DP Controller version 1.2.1.108 (Olympus). For immunohistochemical analysis, the slides were subjected to staining using primary antibodies against PECAM-1, VE-cadherin, β-catenin (all from Santa Cruz Biotechnology, Inc.) followed by biotinylated and peroxidase-conjugated secondary antibodies. They were then processed using the DAB immunostaining assay kit (Santa Cruz Biotechnology, Inc.) according to the instructions. The samples were usually counterstained with hematoxylin before mounting on coverslips.

For the whole-mount staining with anti–PECAM-1 antibody, embryos were fixed in 4% PFA/PBS. After dehydration by a series of methanol, they were treated with 1% H_2O_2 (diluted in MeOH and DMSO mixed 4:1) to quench endogenous peroxidases. Samples were rehydrated by methanol to PBS and blocked in 4% BSA with 0.1% Triton X-100 in PBS. They were then incubated with anti–PECAM-1 (rat monoclonal MEC13.3; 1:50 dilution; BD) diluted 1:10 in 4% BSA in PBS + 0.05% Tween at 4°C

overnight followed by peroxidase-conjugated secondary antibodies. The embryos were developed in 0.25% DAB with H_2O_2 in PBS. They were examined and photographed on a dissecting microscope (model S6D; Leica) with a progressive 3CCD camera (Sony) and Image-Pro Plus version 3.0.00.00 at RT.

Culture of ECs and adenovirus infection

Primary ECs from hearts and lungs of $FAK^{flox/flox}$, $FAK^{+/flox}$, and $FAK^{flox/KD}$ mice were isolated using magnetic bead (Dynabead M-450; Invitrogen) purification with rat anti–mouse PECAM-1 (BD), as described previously (Peng et al., 2004; Shen et al., 2005). In brief, lungs and hearts were harvested, minced, and then digested with 2 mg/ml of type I collagenase (Worthington Biomedical) at 37°C for 45 min. The digested tissue was mechanically dissociated using vigorous flushing through a metal cannula, passed through a 70-µm filter (BD), and then centrifuged at 400 *g* for 8 min at 4°C. The cells were resuspended in cold Dulbecco's PBS and then incubated with rat anti–murine CD31 (PECAM-1; clone MEC 13.3; BD)–coated magnetic beads (M-450; sheep anti–rat IgG Dynabeads; Invitrogen) at 15 µl/ml for 10 min at RT. The beads were washed several times in cold isolation medium (high glucose Dulbecco's modified Eagle's medium containing 20% fetal bovine serum, penicillin, streptomycin [at standard concentrations], and 0.02 M Hepes), resuspended in growth medium (isolation medium supplemented with 100 µg/ml heparin, 100 µg/ml EC mitogen [Biomedical Technologies], L-glutamine, nonessential amino acids, and Na pyruvate at standard concentrations), and cultured in 0.1% gelatin (Sigma-Aldrich)-coated 100-mm tissue culture dishes at 37°C in 5% CO_2.

The recombinant adenoviruses encoding Cre recombinase or lacZ control were purchased from Gene Transfer Vector Core (University of Iowa, Iowa City, IA) and used to infect the primary ECs as described previously (Shen et al., 2005). For most experiments, 10^8 plaque-forming units were used for 10-cm dishes. To increase efficiency, a second infection was performed after 9–12 h. The recombinant adenoviruses encoding FRNK (Ad-FRNK) or GPF control (Ad-GFP) were generated using the AdEasy-1 system (Agilent Technologies) according to manufacturer's instruction. No detectable cell toxicity was observed.

Western blotting

Lysates from primary ECs were prepared and analyzed by Western blotting analysis as described previously (Peng et al., 2004; Shen et al., 2005). In brief, ECs isolated from mice were washed three times with ice-cold PBS and then lysed with modified radioimmunoprecipitation assay buffer (50 mM Tris–HCl, pH 7.5, 150 mM NaCl, 1% NP-40, 1% Na deoxycholate, 1 mM Na vanadate, 10 mM Na pyrophosphate, 10 mM NaF, 1% Triton X-100, 0.5% SDS, 0.1% EDTA, 10 µg/ml leupeptin, 10 µg/ml aprotinin, and 1 mM PMSF). Lysates were cleared by centrifugation, and total protein concentrations were determined using the Bio-Rad Laboratories protein assay. Antibodies used were anti-FAK, anti–phospho-tyrosine397–FAK, anti-Pyk2, anti-p21, anti-p53, anti-Myc, anti–VE-cadherin, and antiactin (all from Santa Cruz Biotechnology, Inc.); anti–phospho-tyrosine402–Pyk2, anti–phospho-serine473–Akt, and anti–phospho-tyrosine417–Src (all from Cell Signaling Technology); and anti–phospho-tyrosine658–VE-cadherin (Biosource International).

TUNEL assay

For detection of apoptotic cells in vivo, paraffin-embedded embryo sections (6 µm) were deparaffinized, incubated in methanol containing 0.3% H_2O_2 for 30 min, washed, and incubated with 20 µg/ml proteinase K in PBS for 15 min at RT. Apoptotic cells were detected as described in the ApopTag Peroxidase In Situ Apoptosis Detection kit (Millipore). In brief, equilibration buffer was applied on each slide for 20 s. After taping off excess liquid, all slides were incubated at 37°C with TdT enzyme for 1 h. The reaction was stopped by stop/wash buffer. The slides were then incubated with antidigoxigenin peroxidase conjugate at RT for 30 min. The staining was made by DAB for 5 min, and the counterstaining was made by methyl green. The slides were examined under a BX41 microscope with UplanF1 10× NA 0.3 objective lens at RT, and the images were captured using a DP70 camera with DP Controller version 1.2.1.108.

For detection of apoptosis of primary ECs infected with Ad-lacZ or Ad-Cre in vitro, the cells were fixed and analyzed using In situ Cell Death Detection kit, TMR red (Roche), according to the manufacturer's instructions. In brief, cells were fixed in 4% PFA in PBS, pH 7.4, for 1 h at RT, followed by incubation in 0.1% Triton X-100 in 0.1% Na citrate for 2 min on ice. Cells were rinsed with PBS, and an aliquot of TUNEL reaction mixture was placed, followed by incubation for 1 h at 37°C in humidified atmosphere in the dark. After washing with PBS, the nuclei were counterstained with Hoechst. Samples were embedded with antifade and subjected to observation under a BX41 microscope with a UplanF1 20× NA 0.5 objective lens at RT. The images were captured using a DP70 camera with DP Controller version 1.2.1.108.

Transwell permeability assay

Permeability across the EC monolayer was measured by using type I collagen–coated Transwell units (6.5-mm diameter and 3.0-µm pore size polycarbonate filter; Corning), essentially as described previously (Moldobaeva and Wagner, 2002). In brief, ECs infected with adenovirus were plated at 10^5 cells in each well and cultured for 2 d to get confluent before experiments. After cells were serum starved in medium 199 containing 1% BSA for 1 h, permeability was measured by adding 1 mg of FITC-labeled dextran (molecular weight, 42,000)/ml to the upper chamber. After incubation for 30 min, 50 µl of sample from the lower compartment was diluted with 300 µl PBS and measured for fluorescence at 520 nm when excited at 492 nm with a spectrophotometer (Synergy HT; BioTek).

Immunofluorescence staining

ECs infected with Ad-lacZ or Ad-Cre were processed for immunofluorescence staining using anti–VE-cadherin (BD) or β-catenin or p120-catenin (both from Santa Cruz Biotechnology, Inc.), as described previously (Shen et al., 2005). Texas red–conjugated mouse anti–rat IgG (1:200), FITC-conjugated goat anti–rabbit IgG (1:200), and FITC-conjugated goat anti–mouse IgG (1:200) were used as the secondary antibodies. They were then mounted on Slowfade (Invitrogen) and examined under a BX41 microscope with a UplanF1 20× NA 0.5 objective lens at RT. The images were captured using a DP70 camera with DP Controller version 1.2.1.108. For detection of EC apoptosis in vivo, brain sections were subjected to TUNEL assay as described above, followed by immunofluorescent staining using anti–PECAM-1 and Hoechst. Images of stained sections were captured using a laser-scanning confocal microscope (FluoView 500; Olympus) and a CCD camera at RT.

Online supplemental material

Fig. S1 shows generation of the KD FAK knockin allele. Fig. S2 shows analysis of embryonic liver sections in vivo and preparation and analysis of primary ECs in vitro. Fig. S3 shows whole-mount analysis of embryos and immunofluorescent staining of isolated primary ECs. Online supplemental material is available at http://www.jcb.org/cgi/content/full/jcb.200912094/DC1.

We are grateful to Drs. T. Saunders and E. Wilkinson (University of Michigan, Ann Arbor, MI) for advice on the generation of knockin mice and analysis of vascular defects, respectively, and to A. Serna for technical assistance. We also thank our laboratory members for helpful comments. We acknowledge E. Hughes, Y.Y. Qu, K. Childs, and G. Gavrilina for the preparation of gene-targeted mice and the University of Michigan Biomedical Research Core Facility, which was supported in part by the University of Michigan Comprehensive Cancer Center (CA046592).

This research was supported by National Institutes of Health grant HL073394 to J.L. Guan.

Submitted: 15 December 2009
Accepted: 13 May 2010

References

Allingham, M.J., J.D. van Buul, and K. Burridge. 2007. ICAM-1-mediated, Src- and Pyk2-dependent vascular endothelial cadherin tyrosine phosphorylation is required for leukocyte transendothelial migration. *J. Immunol.* 179:4053–4064.

Braren, R., H. Hu, Y.H. Kim, H.E. Beggs, L.F. Reichardt, and R. Wang. 2006. Endothelial FAK is essential for vascular network stability, cell survival, and lamellipodial formation. *J. Cell Biol.* 172:151–162. doi:10.1083/jcb.200506184

Chan, P.C., J.F. Lai, C.H. Cheng, M.J. Tang, C.C. Chiu, and H.C. Chen. 1999. Suppression of ultraviolet irradiation-induced apoptosis by overexpression of focal adhesion kinase in Madin-Darby canine kidney cells. *J. Biol. Chem.* 274:26901–26906. doi:10.1074/jbc.274.38.26901

Chiang, Y.J., H.K. Kole, K. Brown, M. Naramura, S. Fukuhara, R.J. Hu, I.K. Jang, J.S. Gutkind, E. Shevach, and H. Gu. 2000. Cbl-b regulates the CD28 dependence of T-cell activation. *Nature*. 403:216–220. doi:10.1038/35003235

Cohen, L.A., and J.L. Guan. 2005. Mechanisms of focal adhesion kinase regulation. *Curr. Cancer Drug Targets*. 5:629–643. doi:10.2174/156800905774932798

Corsi, J.M., C. Houbron, P. Billuart, I. Brunet, K. Bouvrée, A. Eichmann, J.A. Girault, and H. Enslen. 2009. Autophosphorylation-independent and -dependent functions of focal adhesion kinase during development. *J. Biol. Chem.* 284:34769–34776. doi:10.1074/jbc.M109.067280

Dejana, E., F. Orsenigo, and M.G. Lampugnani. 2008. The role of adherens junctions and VE-cadherin in the control of vascular permeability. *J. Cell Sci.* 121:2115–2122. doi:10.1242/jcs.017897

Dvorak, H.F. 2003. Rous-Whipple Award Lecture. How tumors make bad blood vessels and stroma. *Am. J. Pathol.* 162:1747–1757.

Esser, S., M.G. Lampugnani, M. Corada, E. Dejana, and W. Risau. 1998. Vascular endothelial growth factor induces VE-cadherin tyrosine phosphorylation in endothelial cells. *J. Cell Sci.* 111:1853–1865.

Folkman, J. 1995. Seminars in Medicine of the Beth Israel Hospital, Boston. Clinical applications of research on angiogenesis. *N. Engl. J. Med.* 333:1757–1763. doi:10.1056/NEJM199512283332608

Fotedar, R., H. Brickner, N. Saadatmandi, T. Rousselle, L. Diederich, A. Munshi, B. Jung, J.C. Reed, and A. Fotedar. 1999. Effect of p21waf1/cip1 transgene on radiation induced apoptosis in T cells. *Oncogene*. 18:3652–3658. doi:10.1038/sj.onc.1202693

Frisch, S.M., K. Vuori, E. Ruoslahti, and P.Y. Chan-Hui. 1996. Control of adhesion-dependent cell survival by focal adhesion kinase. *J. Cell Biol.* 134:793–799. doi:10.1083/jcb.134.3.793

Gavard, J., and J.S. Gutkind. 2006. VEGF controls endothelial-cell permeability by promoting the beta-arrestin-dependent endocytosis of VE-cadherin. *Nat. Cell Biol.* 8:1223–1234. doi:10.1038/ncb1486

Halder, J., Y.G. Lin, W.M. Merritt, W.A. Spannuth, A.M. Nick, T. Honda, A.A. Kamat, L.Y. Han, T.J. Kim, C. Lu, et al. 2007. Therapeutic efficacy of a novel focal adhesion kinase inhibitor TAE226 in ovarian carcinoma. *Cancer Res.* 67:10976–10983. doi:10.1158/0008-5472.CAN-07-2667

Hunter, T. 2009. Tyrosine phosphorylation: thirty years and counting. *Curr. Opin. Cell Biol.* 21:140–146. doi:10.1016/j.ceb.2009.01.028

Kendall, S.K., L.C. Samuelson, T.L. Saunders, R.I. Wood, and S.A. Camper. 1995. Targeted disruption of the pituitary glycoprotein hormone alpha-subunit produces hypogonadal and hypothyroid mice. *Genes Dev.* 9:2007–2019. doi:10.1101/gad.9.16.2007

Koni, P.A., S.K. Joshi, U.A. Temann, D. Olson, L. Burkly, and R.A. Flavell. 2001. Conditional vascular cell adhesion molecule 1 deletion in mice: impaired lymphocyte migration to bone marrow. *J. Exp. Med.* 193:741–754. doi:10.1084/jem.193.6.741

Lakso, M., J.G. Pichel, J.R. Gorman, B. Sauer, Y. Okamoto, E. Lee, F.W. Alt, and H. Westphal. 1996. Efficient in vivo manipulation of mouse genomic sequences at the zygote stage. *Proc. Natl. Acad. Sci. USA*. 93:5860–5865. doi:10.1073/pnas.93.12.5860

Lampugnani, M.G., M. Corada, L. Caveda, F. Breviario, O. Ayalon, B. Geiger, and E. Dejana. 1995. The molecular organization of endothelial cell to cell junctions: differential association of plakoglobin, beta-catenin, and alpha-catenin with vascular endothelial cadherin (VE-cadherin). *J. Cell Biol.* 129:203–217. doi:10.1083/jcb.129.1.203

Lampugnani, M.G., A. Zanetti, F. Breviario, G. Balconi, F. Orsenigo, M. Corada, R. Spagnuolo, M. Betson, V. Braga, and E. Dejana. 2002. VE-cadherin regulates endothelial actin activating Rac and increasing membrane association of Tiam. *Mol. Biol. Cell*. 13:1175–1189. doi:10.1091/mbc.01-07-0368

Lim, S.T., X.L. Chen, Y. Lim, D.A. Hanson, T.T. Vo, K. Howerton, N. Larocque, S.J. Fisher, D.D. Schlaepfer, and D. Ilic. 2008. Nuclear FAK promotes cell proliferation and survival through FERM-enhanced p53 degradation. *Mol. Cell*. 29:9–22. doi:10.1016/j.molcel.2007.11.031

Moldobaeva, A., and E.M. Wagner. 2002. Heterogeneity of bronchial endothelial cell permeability. *Am. J. Physiol. Lung Cell. Mol. Physiol.* 283:L520–L527.

Parsons, J.T. 2003. Focal adhesion kinase: the first ten years. *J. Cell Sci.* 116:1409–1416. doi:10.1242/jcs.00373

Pawson, T., and M. Kofler. 2009. Kinome signaling through regulated protein-protein interactions in normal and cancer cells. *Curr. Opin. Cell Biol.* 21:147–153. doi:10.1016/j.ceb.2009.02.005

Peng, X., H. Ueda, H. Zhou, T. Stokol, T.-L. Shen, A. Alcaraz, T. Nagy, J.-D. Vassalli, and J.-L. Guan. 2004. Overexpression of focal adhesion kinase in vascular endothelial cells promotes angiogenesis in transgenic mice. *Cardiovasc. Res.* 64:421–430. doi:10.1016/j.cardiores.2004.07.012

Potter, M.D., S. Barbero, and D.A. Cheresh. 2005. Tyrosine phosphorylation of VE-cadherin prevents binding of p120- and beta-catenin and maintains the cellular mesenchymal state. *J. Biol. Chem.* 280:31906–31912. doi:10.1074/jbc.M505568200

Roberts, W.G., E. Ung, P. Whalen, B. Cooper, C. Hulford, C. Autry, D. Richter, E. Emerson, J. Lin, J. Kath, et al. 2008. Antitumor activity and pharmacology of a selective focal adhesion kinase inhibitor, PF-562,271. *Cancer Res.* 68:1935–1944. doi:10.1158/0008-5472.CAN-07-5155

Schaller, M.D. 2001. Biochemical signals and biological responses elicited by the focal adhesion kinase. *Biochim. Biophys. Acta*. 1540:1–21. doi:10.1016/S0167-4889(01)00123-9

Schlaepfer, D.D., and S.K. Mitra. 2004. Multiple connections link FAK to cell motility and invasion. *Curr. Opin. Genet. Dev.* 14:92–101. doi:10.1016/j.gde.2003.12.002

Sekiguchi, T., and T. Hunter. 1998. Induction of growth arrest and cell death by overexpression of the cyclin-Cdk inhibitor p21 in hamster BHK21 cells. *Oncogene*. 16:369–380. doi:10.1038/sj.onc.1201539

Shen, T.L., A.Y. Park, A. Alcaraz, X. Peng, I. Jang, P. Koni, R.A. Flavell, H. Gu, and J.L. Guan. 2005. Conditional knockout of focal adhesion kinase in endothelial cells reveals its role in angiogenesis and vascular development in late embryogenesis. *J. Cell Biol.* 169:941–952. doi:10.1083/jcb.200411155

Siesser, P.M., and S.K. Hanks. 2006. The signaling and biological implications of FAK overexpression in cancer. *Clin. Cancer Res.* 12:3233–3237. doi:10.1158/1078-0432.CCR-06-0456

Skarnes, W.C. 2000. Gene trapping methods for the identification and functional analysis of cell surface proteins in mice. *Methods Enzymol.* 328:592–615. doi:10.1016/S0076-6879(00)28420-6

Slack-Davis, J.K., K.H. Martin, R.W. Tilghman, M. Iwanicki, E.J. Ung, C. Autry, M.J. Luzzio, B. Cooper, J.C. Kath, W.G. Roberts, and J.T. Parsons. 2007. Cellular characterization of a novel focal adhesion kinase inhibitor. *J. Biol. Chem.* 282:14845–14852. doi:10.1074/jbc.M606695200

Sonoda, Y., Y. Matsumoto, M. Funakoshi, D. Yamamoto, S.K. Hanks, and T. Kasahara. 2000. Anti-apoptotic role of focal adhesion kinase (FAK). Induction of inhibitor-of-apoptosis proteins and apoptosis suppression by the overexpression of FAK in a human leukemic cell line, HL-60. *J. Biol. Chem.* 275:16309–16315. doi:10.1074/jbc.275.21.16309

Turowski, P., R. Martinelli, R. Crawford, D. Wateridge, A.P. Papageorgiou, M.G. Lampugnani, A.C. Gamp, D. Vestweber, P. Adamson, E. Dejana, and J. Greenwood. 2008. Phosphorylation of vascular endothelial cadherin controls lymphocyte emigration. *J. Cell Sci.* 121:29–37. doi:10.1242/jcs.022681

Watson, E.D., and J.C. Cross. 2005. Development of structures and transport functions in the mouse placenta. *Physiology (Bethesda)*. 20:180–193.